Supporting Information

Lee et al. 10.1073/pnas.0904408106

SI Text

Cell Growth and Protein Purification. *A. vinelandii* strain YM13A (expressing His-tagged MoFe protein) and YM68A (expressing His-tagged VFe protein) were grown in 180-l batches in a 200-l New Brunswick fermentor (New Brunswick Scientific) in Burke's minimal medium supplemented with 2 mM ammonium acetate [Note that the Mo in Burke's medium was replaced by an equal amount of V for the growth of YM68A strain]. The growth rate was measured by cell density at 436 nm using a Spectronic 20 Genesys. Cells were harvested in the late exponential phase by using a flow-through centrifugal harvester (Cepa). The cell paste was washed with a buffer containing 50 mM Tris·HCl (pH 8.0). Published methods were used for the purification of His-tagged MoFe and VFe proteins (1, 2), and nontagged *nifH*- and *vnfH*-encoded Fe proteins (3).

Protein Characterization. Native PAGE of MoFe and VFe proteins was performed in a Vacuum Atmospheres dry box at an oxygen level of <4 ppm. Precast gels (Bio-Rad) were prerun in an anaerobic running buffer with 2 mM $Na_2S_2O_4$ at 80 V for 1 h before the loading of protein samples. Native molecular weight of VFe protein was determined by Sephacryl S-300 HR gel filtration (General Electric Healthcare) with conalbumin (75 kDa), aldolase (158 kDa), ferritin (440 kDa), and thyroglobulin (669 kDa) as protein standards. To determine the stoichiometry of the VFe protein, subunits were first separated by SDS/PAGE and subsequently transferred onto a PVDF membrane. Coomassie blue staining was performed on both the gel and the membrane afterward to ensure complete and even transfer. The membrane was analyzed by the Molecular Structure Facility at the University of California at Davis for total amino acid composition of each subunit.

Activity Assays and Metal Analysis. Iron was determined as published (4). Vanadium was determined by a published method (5) after the protein was ashed in H_2SO_4 at 440 °C for 2 h. All nitrogenase activity assays were carried out as described (2, 3). The products H_2, C_2H_4 and C_2H_6 were analyzed as described elsewhere (6). Ammonium was determined by a high-performance liquid chromatography fluorescence method (7).

EPR Spectroscopy. All EPR samples were prepared in a Vacuum Atmospheres dry box at an oxygen level of <4 ppm. Unless noted otherwise, all samples were in 25 mM Tris·HCl (pH 8.0), 10% glycerol, and 2 mM $Na_2S_2O_4$. Oxidized VFe protein samples were prepared by incubation with excess IDS for 5 min. All perpendicular-mode and parallel-mode EPR spectra were recorded by using a Bruker ESP 300 E_z spectrophotometer (Bruker) interfaced with an Oxford Instruments ESR-9002 liquid helium continuous-flow cryostat. Unless noted otherwise, all spectra were recorded by using a microwave power of 50 mW, a gain of 5×10^4, a modulation frequency of 100 kHz, and a modulation amplitude of 5 G. The microwave frequencies of 9.62 and 9.39 GHz were used for the perpendicular-mode (5 scans) and parallel-mode (10 scans) EPR spectra, respectively. Temperatures at which the spectra were taken are indicated in *Results*. Spin quantitation of EPR signals was carried out as described (2). EPR turnover samples were prepared as described (8, 9) and contained 15 mg VFe protein, 0.8 mg *vnfH*-encoded Fe protein, 6 mM Na_2ATP, 8 mM $MgCl_2$, 50 mM phosphocreatine, 0.20 mg/mL creatine phosphokinase, 20 mM $Na_2S_2O_4$, and 25 mM Tris·HCl (pH 8.0).

1. Ribbe MW, Hu Y, Guo M, Schmid B, Burgess BK (2002) The FeMoco-deficient MoFe protein produced by a *nifH* deletion strain of *Azotobacter vinelandii* shows unusual P-cluster features. *J Biol Chem* 277:23469–23476.
2. Hu Y, Fay AW, Dos Santos PC, Naderi F, Ribbe MW (2004) Characterization of *Azotobacter vinelandii nifZ* deletion strains: Indication of stepwise MoFe protein assembly. *J Biol Chem* 279:54963–54971.
3. Burgess BK, Jacobs DB, Stiefel EI (1980) Large-scale purification of high activity *Azotobacter vinelandii* nitrogenase. *Biochim Biophys Acta* 614:196–209.
4. Van de Bogart M, Beinert H (1967) Micro methods for the quantitative determination of iron and copper in biological material. *Anal Biochem* 20:325–334.
5. Fishman MJ, Skougstad MV (1964) Catalytic determination of vanadium in water. *Anal Chem* 36:1643–1647.
6. Gavini N, Burgess BK (1992) FeMo cofactor synthesis by a *nifH* mutant with altered MgATP reactivity. *J Biol Chem* 267:21179–21186.
7. Corbin JL (1984) Liquid chromatographic-fluorescence determination of ammonia from nitrogenase reactions: A 2-min assay. *Appl Environ Microbiol* 47:1027–1030.
8. Benton PM, et al. (2003) Localization of a substrate binding site on the FeMo-cofactor in nitrogenase: Trapping propargyl alcohol with an α-70-substituted MoFe protein. *Biochemistry* 42:9102–9109.
9. Maskos Z, Fisher K, Sørlie M, Newton WE, Hales BJ (2005) Variant MoFe proteins of *Azotobacter vinelandii*: Effects of carbon monoxide on electron paramagnetic resonance spectra generated during enzyme turnover. *J Biol Inorg Chem* 10:394–406.

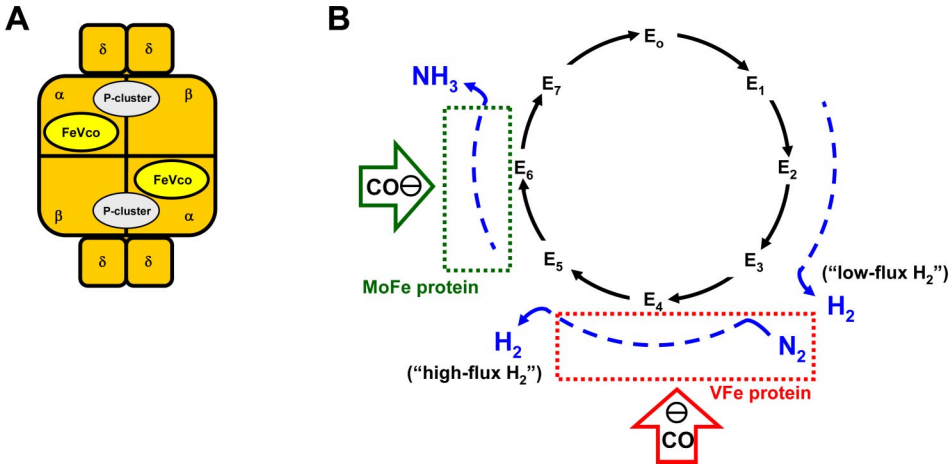

Fig. S1. Plausible structure of VFe protein and its CO inhibition mechanism. (*A*) Schematic presentation of the $\alpha_2\beta_2\delta_4$-heterooctameric VFe protein. The δ-subunits may exist as 2 pairs of δ_2 dimers, each locating at the interface of 1 α/β-subunit pair. (*B*) Proposed mechanism of CO inhibition on H_2 evolution by MoFe and VFe proteins. Shown is a simplified Lowe–Thorneley model depicting the coproduction of NH_3 and H_2 by MoFe protein under N_2. E_n represents a functional enzymatic unit of nitrogenase, which has been reduced by n electrons. Under high electron flux, N_2 can bind at either E_3 or E_4 state, and this process is accompanied by H_2 evolution (high-flux H_2). The reductive cycle continues beyond the E_3 or E_4 state and NH_3 is released later, likely before the E_7 state, after which the enzyme is converted back to the E_0 state and ready for the next round of turnover. Under low electron flux, however, the enzyme cannot go beyond a certain reductive state, such as the E_3 or E_4 state. Consequently, N_2 cannot bind to the enzyme and the electrons are used for H_2 evolution that is not associated with N_2 binding and reduction (low-flux H_2). In the case of the MoFe protein, CO likely interferes at a later stage, likely where NH_3 is produced and/or released (green box). Therefore, the formation of NH_3 cannot be detected, yet the production of H_2 is unaffected. If the VFe protein follows a reaction mechanism similar to that of the MoFe protein, CO may interfere at an earlier stage, likely before or after the binding of N_2 (red box). As a result, formation of the high-flux H_2 is inhibited concomitantly with the binding and/or reduction of N_2, yet the low-flux H_2 can still be generated.